SF-98-10-3 (4107)

# Numerical Simulation of Airflow in a Room with Differentially Heated Vertical Walls

**Weiran Xu**
Student Member ASHRAE

**Qingyan Chen, Ph.D.**
Member ASHRAE

## ABSTRACT

*Knowledge of room air distribution, including its flow and temperature characteristics, is very important to HVAC engineers. This study numerically predicts the air distribution in a room with differentially heated vertical walls. The Rayleigh number in the room is around $2.6\sim3\times10^{10}$. Time averaged equations of continuity, momentum, and energy are numerically solved by the finite volume method. Three turbulence models, the "standard" k-ε model, and two low-Reynolds-number k-ε models, are employed to simulate turbulent natural convection in the room. The numerical results are compared with experimental data available and other related work. Good agreement occurs between the numerical results and the experimental data. Low-Reynolds-number effects and thermal radiation between the ceiling and floor are found to have important impacts on the flow pattern and the temperature distribution.*

## INTRODUCTION

### Statement of the Problem

The temperature distribution and flow features within a room have a significant influence on the health and thermal comfort of occupants. Indoor air quality (IAQ) problems such as *sick building syndrome* have attracted more and more attention in recent years. On the other hand, the velocity of airflow, temperature distribution of room air, and turbulence intensities are directly related to the thermal comfort of occupants. Thus, knowledge of flow and temperature fields is essential to HVAC engineers in order to design a good ventilation system.

The detailed knowledge of air distribution can be obtained by using computational fluid dynamics (CFD). Since most airflows in rooms are turbulent and the physics of turbulence is not well understood, engineers in turn apply so-called turbulence models in the CFD. Because turbulence models are approximated methods, they need to be validated by experimental data before being used as a design tool. Some researchers have made efforts to measure the airflows in the real rooms or use a small-scale model to represent a full-scale room (Olson et al. 1990). However, both experimental approaches are much more expensive than using the CFD technique and lack the flexibility to simulate various boundary conditions such as a complex diffuser. With the CFD technique, whole field distribution can be obtained from the solutions, while in most experiments the measurements can only be carried out in a few locations of the room.

Room airflows can be classified as forced convection, natural convection, or mixed convection. This paper will attack the problems of the natural convection in a room with differentially heated vertical walls by using the CFD technique with turbulence models.

### Previous Work

Related studies on natural convection in rooms take either experimental or numerical approaches. De Vahl Davis et al. (1984) organized a workshop of numerical simulation on natural convection in a square cavity with the Rayleigh number from $10^3$ to $10^6$. They compared results of the average Nusselt number, the local Nusselt number, the maximum velocity on the hot wall, and other relevant quantities from different contributors. They found the finite element method performed well in low-Rayleigh-number cases but not in high-Rayleigh-number cases. On the other hand, the finite difference method seemed approximately independent of a Rayleigh number.

Ball and Bergman (1993) used the Chebyshev collocation technique to calculate the enclosures with differentially heated side walls. They calculated enclosures with a different aspect ratio and a range of Ra up to $10^6$. Oscillatory convection was found when Ra exceeded a certain value.

Henkes et al. (1991) presented a numerical simulation of natural convection in a square cavity. Low-Reynolds-number models were used to study flows with Rayleigh numbers up to

**Weiran Xu** is a doctoral student and **Qingyan Chen** is an assistant professor in the Building Technology Program, Department of Architecture, Massachusetts Institute of Technology, Cambridge.

$10^{14}$. They found that the position of laminar-turbulence transition in the vertical boundary layer highly depends on the turbulence model used. The same Rayleigh number and grid could produce multiple solutions.

Henkes et al. (1995) compared numerical results on natural convection in a square cavity obtained from ten research groups. The Rayleigh number studied is $5\times10^{10}$. The standard $k$-$\varepsilon$ turbulence model was used for the comparison of numerical accuracy. The heat transfer rate is found to be overpredicted by the standard $k$-$\varepsilon$ model.

Paolucci (1990) presented a direct numerical simulation of turbulent natural convection in a square cavity with a Rayleigh number of $10^{10}$. His results were confirmed by the experimental data. From the computational results, he displayed the formation of the turbulent natural convection from the initial instability of air in the cavity. This study gave some basic understanding of the natural convection in enclosures.

Cheesewright et al. (1986) measured natural convection in a cavity with a Rayleigh number of $5\times10^{10}$. Air velocities, temperatures, and turbulence quantities were measured. They presented a method to correct the influences of the heat loss from walls due to imperfect insulation. The nonsymmetrical boundary layer on the hot and cold wall and relaminarisation at the bottom of the hot-wall boundary were found. This experiment was numerically simulated by Chen et al. (1990).

Olson et al. (1990) measured the natural convection in a full-scale room as well as in a small-scale model with differentially heated walls. The aspect ratio of the room, H/L, is around 0.3. Figure 1a shows the configuration of their experiment. This is a case very close to a real room. They found turbulent boundary layers on vertical walls and wandering flow in the core region. These features were not found in previous studies on natural convection in enclosures. This is a very challenging phenomenon that should be studied.

Few studies have simulated natural convection in a real room with a Rayleigh number close to the reality. In this study, we aim at the prediction of the distributions of velocity, temperature, and turbulence quantities for the natural convection in the room. The experimental data (Olson et al. 1990) will be used to verify the accuracy of numerical results. Other important factors, such as the effects of radiation on airflow between the ceiling and floor, are also discussed.

## MATHEMATICAL DESCRIPTION

From the previous review, the CFD technique seems to be an appropriate tool for the study of natural convection in rooms. This section briefly discusses the CFD technique.

### Governing Equations

The CFD technique solves conservation equations of mass, momentum, and energy. Since room airflows are turbulent, the turbulent natural convection is inherently time-dependent and three-dimensional. In our case, the flow is assumed to be two-dimensional since the width is sufficiently large, so that the end effect can be safely neglected. The experiment conducted by Olson et al. (1990) confirmed that the flow can be further assumed to be steady. Finally, the Boussinesq assumption for buoyancy that treats density as a constant and considers buoyancy effects in momentum equation is used. Conservation equations of mass, momentum, and energy are well known, so only formulas of turbulence models appear below.

Based on the above analysis, the general form of $k$-$\varepsilon$ model equations reads

$$\frac{\partial Uk}{\partial x}+\frac{\partial Vk}{\partial y}=\frac{\partial}{\partial x}\left(\nu+\frac{\nu_t}{\sigma_k}\right)\frac{\partial k}{\partial x}+\frac{\partial}{\partial y}\left(\nu+\frac{\nu_t}{\sigma_k}\right)\frac{\partial k}{\partial y}+P_k-\varepsilon+G_k \quad (1)$$

$$\frac{\partial U\varepsilon}{\partial x}+\frac{\partial V\varepsilon}{\partial y}=\frac{\partial}{\partial x}\left(\nu+\frac{\nu_t}{\sigma_\varepsilon}\right)\frac{\partial \varepsilon}{\partial x}+\frac{\partial}{\partial y}\left(\nu+\frac{\nu_t}{\sigma_\varepsilon}\right)\frac{\partial \varepsilon}{\partial y}+\frac{\varepsilon}{k}(C_{1\varepsilon}f_1P_k-C_{2\varepsilon}f_2\varepsilon)+G_\varepsilon \quad (2)$$

where

$$\nu_t=f_\mu C_\mu\frac{k^2}{\varepsilon}\qquad G_k=\beta\frac{\nu_t}{\sigma_T}\frac{\partial T}{\partial y}g\qquad G_\varepsilon=C_{3\varepsilon}\frac{\varepsilon}{k}G_k \quad (3)$$

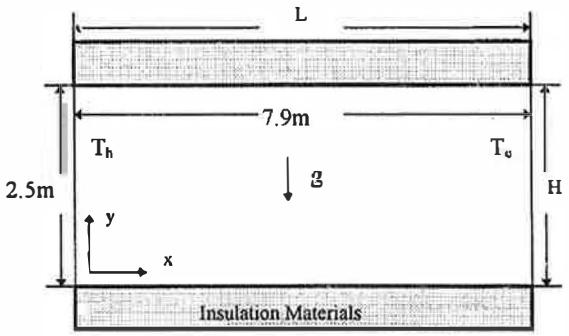


(a)

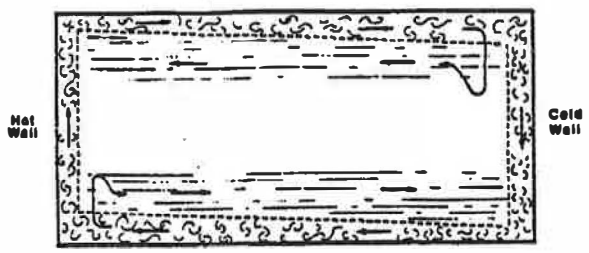


(b)

***Figure 1*** *(a) Sketch of the physical model (Olson et al. 1990); (b) Flow pattern observed by Olson et al. (1990).*

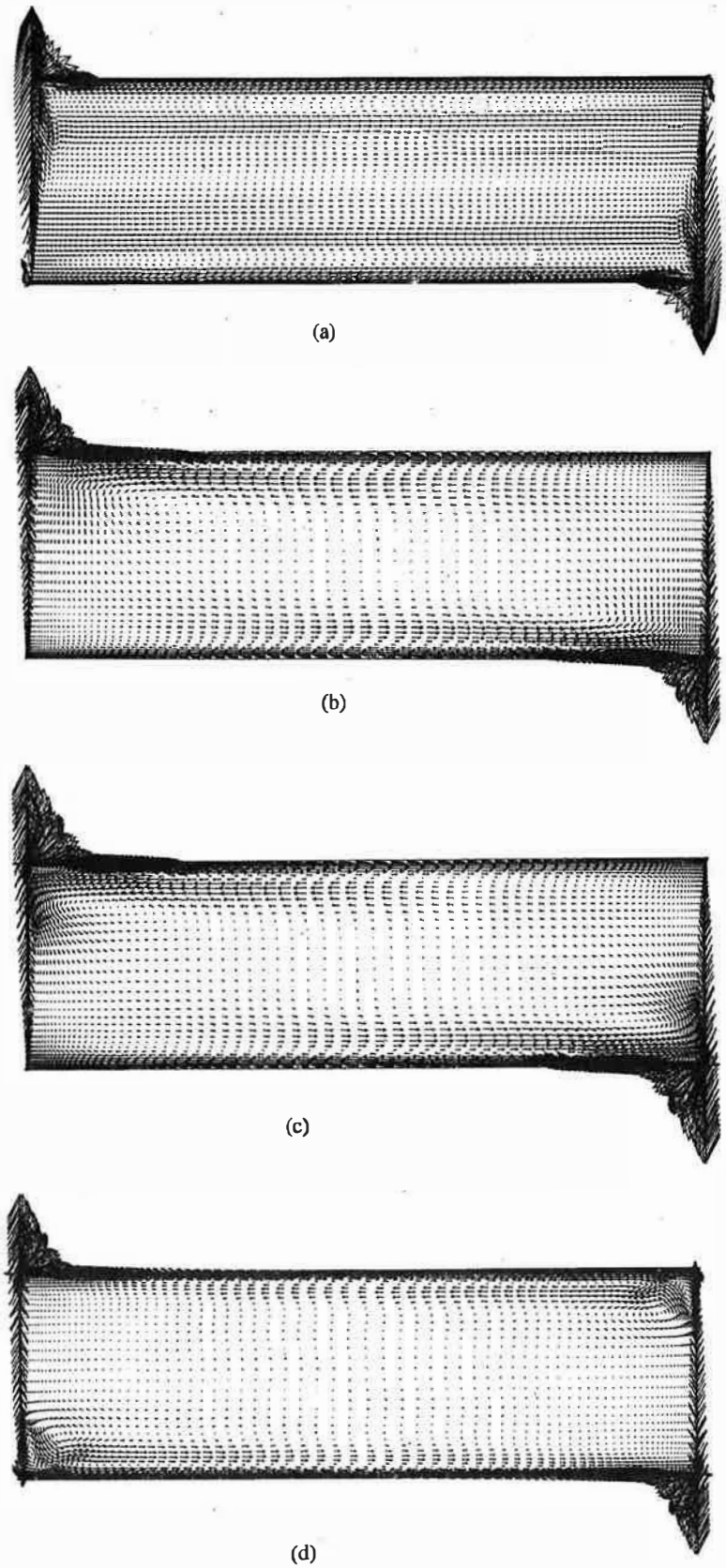


***Figure 2*** *Velocity distribution computed by (a) the standard k-ε model, (b) the LB model, (c) the NT model, and (d) the LB model with inclusion of thermal radiation.*

In this paper, the "standard" $k$-ε model and two low-Reynolds-number models are used. The standard $k$-ε turbulence model is a high-Reynolds-number model that is appropriate in the region away from the walls. In the near-wall vicinity where viscosity is dominant and the overall Reynolds number, $Re_t$, is low, wall functions are often used. Evidence also shows the natural convection in a room has a relatively small $Re_t$ (Chen et al. 1990). The standard $k$-ε model may not be appropriate even in the region far from the walls. One of the alternatives is to use low-Reynolds-number models. Low-Reynolds-number models account for low-Reynolds-number effects by introducing damping factors $f_1$, $f_2$, and $f_m$. These factors become smaller in the near-wall region and approach unity away from the walls. Unfortunately, the application of a low-Reynolds-number model requires more grids close to the walls because of the large gradient of the variables such as $U$, $V$, $T$, $k$, and ε, etc. The following section discusses the differences of these three models.

- Standard $k$-ε model (Launder and Spalding 1974, hereafter denoted as "Standard Model"). This model is a high-Reynolds-number model so that damping functions are set to unity in the general form:

$$f_\mu = f_1 = f_2 = 1$$

The constants used in the model are

$$C_\mu = 0.09 \quad C_{1\varepsilon} = 1.44 \quad C_{2\varepsilon} = 1.92 \quad C_{3\varepsilon} = 1.44$$
$$\sigma_k = 1.0 \quad \sigma_\varepsilon = 1.3 \quad \sigma_T = 1.0 \tag{4}$$

- Lam and Bremhorst low-Reynolds-number $k$-ε model (1981, hereafter denoted as "LB Model") introduces damping functions as

$$f_\mu = [1 - \exp(-0.0165\mathrm{Re}_k)]^2\left(1 + \frac{20.5}{\mathrm{Re}_t}\right)$$
$$f_1 = 1 + \left(\frac{0.05}{f_\mu}\right)^3 \qquad f_2 = 1 - \exp(-\mathrm{Re}_t^2) \tag{5}$$

where $\mathrm{Re}_t = \frac{k^2}{\nu\varepsilon}$. The model constants are the same as those in the standard model:

$$C_\mu = 0.09 \quad C_{1\varepsilon} = 1.44 \quad C_{2\varepsilon} = 1.92 \quad C_{3\varepsilon} = 1.44$$
$$\sigma_k = 1.0 \quad \sigma_\varepsilon = 1.3 \quad \sigma_T = 1.0$$

- Nagano and Tagawa low-Reynolds-number $k$-ε model (1990, hereafter denoted as "NT Model") has different damping functions:

$$f_\mu = \left[1 - \exp\left(-\frac{y^+}{26}\right)\right]^2\left(1 + \frac{4.1}{\mathrm{Re}_t^{3/4}}\right) \qquad f_1 = 1.0$$
$$f_2 = \left[1 - 0.3\exp\left(-\left(\frac{\mathrm{Re}_t}{6.5}\right)^2\right)\right]\left(1 - \exp\left(-\frac{y^+}{6}\right)\right)^2 \tag{6}$$

The model constants are also slightly different:

$$C_\mu = 0.09 \quad C_{1\varepsilon} = 1.45 \quad C_{2\varepsilon} = 1.9 \quad C_{3\varepsilon} = 1.44$$
$$\sigma_k = 1.4 \quad \sigma_\varepsilon = 1.3 \quad \sigma_T = 1.0 \tag{7}$$

### Boundary Conditions

In order to solve the above equations, boundary conditions must also be provided. In the case studied in this paper, two vertical walls are isothermal and two horizontal walls are adiabatic. No-slip boundary conditions are used for velocity at all walls.

For turbulence quantities $k$ and ε, different models require different boundary conditions. For the standard model, wall functions (Launder and Spalding 1974) are desirable. For the LB model and the NT model, two sets of boundary conditions are employed. One set uses $k = 0$, $\frac{\partial \varepsilon}{\partial y} = 0$ at all walls while the other still uses the wall functions but with the first inner grid very close to the wall. The boundary conditions for turbulence quantities usually significantly influence the accuracy, even the convergence, of the numerical simulation.

## NUMERICAL PROCEDURE

In order to obtain numerical solutions, the above differential equations are discretized by using the finite volume method with the staggered grids. Since the conservation equations are nonlinear, iterations are needed to obtain a converged solution. Exponential grid distribution is adopted to increase the spatial resolution near walls since low-Reynolds-number models require very fine grids in the near-wall region. The first grid is arranged in the viscous sublayer, and at least five grids are located within the region of $y^+ < 11.5$.

A commercial software is used as a solver (Spalding 1994). The criterion of convergence is defined as the maximum value of the absolute residuals of the transport equations for $U, V, P, T, k$, ε is less than $10^{-3}$.

## RESULTS AND DISCUSSION

The physical model selected for the investigation is the one used by Olson et al. (1990), as shown in Figure 1a. The prototype is a room with two vertical walls kept in different temperatures while other walls are insulated. The room is 26 ft (7.9 m) in length, 8.2 ft (2.5 m) in height, and 12.8 ft (3.9 m) in width. The temperatures on the hot wall and cold wall are 95.5°F (35.3°C) and 67.8°F (19.9°C), respectively.

### Air Flow Pattern

Figure 1b shows the flow pattern observed in the experiment. Turbulence was found near the vertical walls. Two horizontal flow-loops on the ceiling and floor were also observed.

To simulate the turbulence found in the experiment, three $k$-ε turbulence models were applied (standard model, LB model, and NT model). When the standard model was used with wall functions for $k$ and ε, the first inner grid was placed sufficiently far from the wall to satisfy the requirement for

applying wall functions. Figure 2a illustrates the velocity vector field obtained by the standard model. The results show no recirculations. The reason, although it is difficult to identify, is probably that the standard model cannot handle low-Reynolds-number effects.

The flow pattern observed in the experiment shows a noticeably large eddy at the upper-right and the lower-left corners. Olson et al. (1990) argued this is because the horizontal mass flow on the ceiling is too great to entrain entirely into the cold wall boundary layer. After turning down, the outer portion of the flow goes upwards and forms the eddy and the reverse flow. This suggests that a buoyancy force in the corner regions might be important. Therefore, the variable density method that treats density as a variable in all equations is used to check their argument. Unfortunately, the results from the variable density method show again without the recirculation. Therefore, the authors believe other factors rather than pure buoyancy effects may have contributed to the flow pattern.

From further literature survey and analysis of experimental and previous computational results, turbulence is found weak under the current Rayleigh number and relaminazation often occurs. This suggests that a low-Reynolds-number turbulence model should be used. A low-Reynolds-number model can take the low-Reynolds-number effects into account. Chen (1995) applied several $k$-ε turbulence models for natural convection of room air. He found that the LB low-Reynolds-number model performed the best.

The LB model is thus employed in this study, and recirculating flow on the ceiling and floor appears in the computational results. Figure 2b shows the vector field obtained with the LB model. A similar result alsc occurs with the NT model as shown in Figure 2c. Two sets of boundary conditions for $k$ and ε are tested with the LB model. The results with two boundary conditions are similar. We can conclude that the special recirculating loop is due to the effects of the low-Reynolds-number.

The studies by Henkes et al. (1991) and a workshop (Henkes et al. 1995) introduced the concept of a critical Rayleigh number $Ra_{cr}$. $Ra_{cr}$ is around $10^9$ with high-Reynolds-number models and $10^{11}$ with low-Reynolds-number models. When Ra is lower than $Ra_{cr}$, laminar flow is found. Fully turbulent flow is found with Ra being greater than $10^{14}$. Multi-solutions exist when Ra is between $Ra_{cr}$ and $10^{14}$, which is also the range of transition. These solutions are called *bifurcation branches* of the governing equations. The initial conditions and disturbances have a substantial impact on the solutions.

In our study, the Rayleigh number is around $2.6\sim3\times10^{10}$, that is, just in the regime of transition. Small temperature variations on the vertical walls and heat loss through the ceiling and floor are considered additional disturbances. One possible explanation of the wandering flow pattern in Olson's experiment would be that it is produced by bifurcation. Although the results of the LB and NT models agree with the flow pattern observed in the experiment, it is still not very clear if other low-Reynolds-number models could predict the airflow in this room. Therefore, an extensive testing of other low-Reynolds-number $k$-ε models is recommended in future studies.

It should be noted that in Figures 2c and 2d no eddy appears at the upper-right and lower-left corners of the room. Olson et al. describe the eddies occurring in the experiment as the large mass flow on the ceiling and buoyancy effects. However, thermal radiation between the ceiling and floor that was not considered in the earlier computation may have contributed to the flow pattern. Therefore, a surface-to-surface radiation model is employed to calculate the radiative heat transfer.

Figure 2d shows that the LB model with the inclusion of thermal radiation can predict eddies at the corner as well as the recirculating flow on the ceiling and floor. Clearly, thermal radiation directly contributes to the eddies at the upper-right corner of the cold wall and the lower-left corner of the hot wall. Figure 3 shows the comparison of the surface temperature of the ceiling. The surface temperature with the calcula-

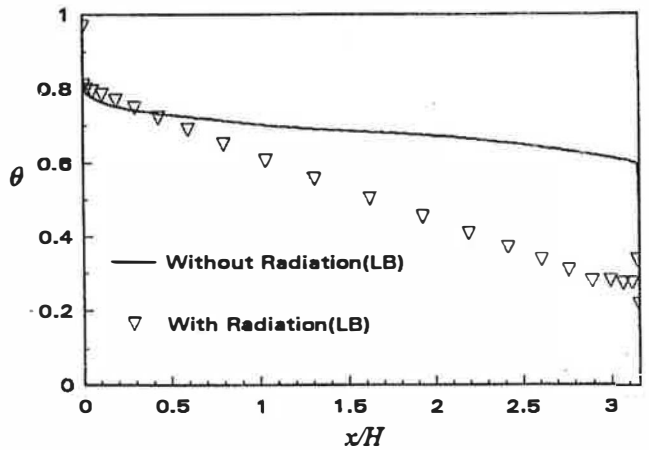


*Figure 3* *Comparison of the computed temperature distribution on the ceiling with and without radiation.*

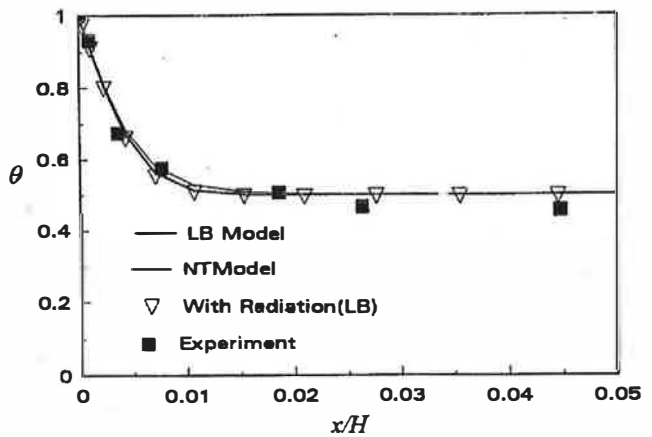


*Figure 4* *Comparison of the computed temperature profile at y=H/2 with the experimental data from Olson et al. (1990).*

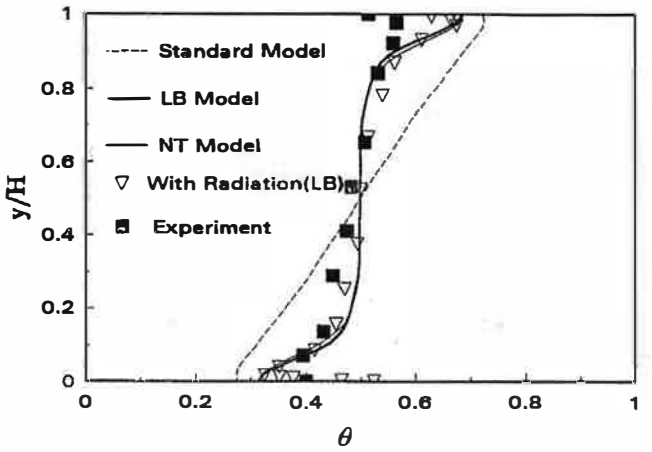


*Figure 5* *Comparison of the computed temperature profile at x=L/2 with the experimental data from Olson et al. (1990).*

tion of radiation is significantly lower than that without radiation considered, especially in the region close to the cold wall. This difference results in more air at the upper-right corner of the room becoming denser. This confirms the explanation given by Olson et al. that the eddies are formed because the "mass flow is too large to entrain entirely into the cold wall boundary layer." (Olson et al. 1990)

The flow pattern predicted with the radiation model is closest to the experiment. This suggests that in natural convection, thermal radiation between walls has a significant impact on air distribution.

## Temperature Profile

Figure 4 shows the comparison of the dimensionless temperature θ along x (horizontal) direction at y = H/2 (mid-height). The predicted temperatures are slightly higher than experimental data. The largest difference is less than 8%, which can also be considered as a good agreement.

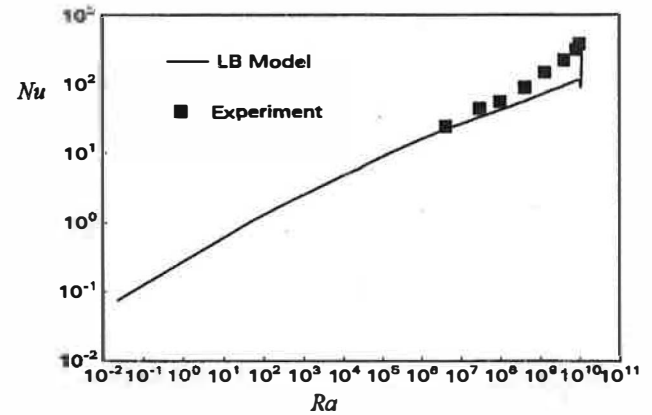


*Figure 6* *Comparison of local Nu versus local Ra on the hot wall with the experimental data from Cheesewright et al. (1986).*

The numerical results of the temperature distribution along the vertical center line are also compared with experimental data in Figure 5. Good agreement is found in the core but not in the near-wall regions when adiabatic conditions are applied in numerical simulations. There are heat losses through the ceiling and floor in the experiments since it is impossible to have ideal adiabatic conditions. Figure 5 also shows that the case with the consideration of thermal radiation agrees better with the experimental data.

## Heat Transfer

The Local Nusselt number along the hot wall is shown in Figure 6. Since the uncertainty of the Nusselt number in the experimental data (Olson et al. 1993) is too large, the computed result is compared with the measurements of a cavity with a Rayleigh number of $5\times10^{10}$ (Cheesewright et al. 1986). In spite of the differences between two cases in terms of geometry and the Rayleigh number, the trends and magnitude agree well.

## Applications

The two-dimensional enclosure with differentially heated vertical walls can be a physical model of many practical applications, such as atriums with large glazing area in cold climates. The results of this study also provide a guideline of selecting turbulence models for the natural convection in rooms. However, it should be noted that though low-Reynolds number models are more accurate, they require significant computation time since large grid numbers are needed in the near-wall region. Efforts should be made in the future to devise a more cost-effective and, thus, more practical method for HVAC engineers.

## CONCLUSION

This study finds suitable turbulence models that can be used to predict the airflow, temperature distribution, and heat transfer in a room with differentially heated vertical walls. Three turbulence models, including the standard $k$-ε model and two low-Reynolds-number models, have been tested. Flow pattern and temperature profile calculated by low-Reynolds-number models agree well with the experimental data (Olson 1990), but the standard $k$-ε model does not. Low-Reynolds-number effects such as bifurcation could be a reason for the recirculations in the airflow pattern. Thermal radiation between the ceiling and floor has an important impact on the flow pattern at the room corners and temperature distribution on the horizontal walls.

## ACKOWLEDGEMENT

The investigation is supported by the US National Science Foundation Grant No. CMS-9623864.

BACK TO PAGE ONE

## NOMENCLATURE

| | | |
|---|---|---|
| $C_{1\varepsilon}, C_{2\varepsilon}, C_{3\varepsilon}, C_\mu$ | = | coefficients in turbulence models |
| $f_1, f_2, f_\mu$ | = | damping functions used in the low-Reynolds-number $k$-$\varepsilon$ models |
| $g$ | = | gravity acceleration |
| $G_k$, $G_\varepsilon$ | = | buoyancy production term in $k$-$\varepsilon$ models |
| $H$ | = | room height |
| $i, j$ | = | spatial direction indices |
| $k$ | = | turbulent kinetic energy |
| $k_c$ | = | thermal conductivity |
| $L$ | = | room length |
| $Nu$ | = | Nusselt number $\frac{Q}{Wk_{air}(T_h - T_c)}$ |
| $P$ | = | mean pressure |
| $Q$ | = | heat transferred through walls |
| Ra | = | Rayleigh number $\frac{g\beta(T_h - T_c)H^3}{\nu\alpha}$, a measure of the strength of the buoyancy effect in fluid |
| Re | = | Reynolds number, the ratio of the inertia force over the viscous force in fluids |
| $\mathrm{Re}_k$ | = | $\frac{\sqrt{k}y_n}{\nu}$ |
| $\mathrm{Re}_t$ | = | $\frac{k^2}{\nu\varepsilon}$ |
| $T$ | = | temperature |
| $T_h$, $T_c$ | = | temperature of hot wall and cold wall |
| $U, V$ | = | mean velocity components in x and y direction |
| $U_T$ | = | wall friction velocity |
| $W$ | = | room width |
| $x, y$ | = | Cartesian coordinates |
| $y_n$ | = | normal distance to nearest wall |
| $y^+$ | = | $\frac{U_t y_n}{\nu}$ |
| Greek symbols | | |
| $\beta$ | = | thermal expansion coefficient |
| $\varepsilon$ | | turbulence dissipation |
| $\rho$ | = | fluid density |
| $\nu$ | = | kinetic viscosity of fluid |
| $\nu_t$ | = | eddy-viscosity |
| $\sigma_k, \sigma_\varepsilon, \sigma_T$ | = | diffusion coefficients in the turbulence models |
| $\sum_{i,j}$ | = | summation of all nodes in the computational domain |

## REFERENCES


Ball, K. S., and T. L. Bergman. 1993. Numerical simulation of unsteady low Pr convection using a Chebyshev collocation technique. ASME Paper: 93-WA/HA-43.

Cheesewright, R., K. J. King, and S. Ziai. 1986. Experimental data for validation of computer codes for prediction of two-dimensional buoyant cavity flows. *Significant questions in buoyancy affected enclosure or cavity flows*, (Ed. by J. A. C. Humphrey, C. T. Adedisian, and B. W. le Tourneau). ASME, pp. 75-81.

Chen, Q., A. Morser, and A. Huber. 1990. Prediction of buoyant, turbulent flow by a low-Reynolds-number $k$-$\varepsilon$ model. *ASHRAE Transactions* 96(1):564-573.

Chen, Q., and Z. Jiang. 1992. Significant questions in predicting room air motion. *ASHRAE Transactions* 98(1):929-939.

Chen, Q. 1995. Comparison of different $k$-$\varepsilon$ models for indoor airflow computations. *Numerical Heat Transfer, Part B* 28:353-369.

Chen, Q. 1996. Prediction of room air motion by Reynolds-stress models. To appear in *Building and Environment*.

De Vahl Davis, G., I. P. Jones. 1984. Natural convection in a square cavity: A comparison exercise. *Int. J. Numer. Methods Fluids* 3:227-248.

Henkes, R. A. W. M., F. F. Van Der Vlugt, and C. J. Hoogendoorn. 1991. Natural convection flow in a square cavity calculated with low-Reynolds-number turbulence model. *Int. J. Heat Mass Transfer, Part B* 28:59-78.

Henkes, R. A. W. M. and C. J. Hoogendoorn. 1995. Comparison exercise for computations of turbulent natural convection in enclosures. *Numerical Heat Transfer, Part B* 28:59-78.

Lam, C. K. G., and K. A. Bremhorst. 1981. Modified form of $k$-$\varepsilon$ model for predicting wall turbulence. *J. Fluids Engng, ASME Trans.* 103:456-460.

Launder, B. E., and D. B. Spalding. 1974. The numerical computation of turbulent flows. *Computer Methods in Applied Mechanics and Energy* 3:269-289.

Morser, A., F. Off, A. Schalin, and X. Yuan. 1995. Numerical modeling of heat transfer by radiation and convection in an atrium with thermal inertia. *ASHRAE Transactions* 101(2):1136-1143.

Nagano, Y., and M. Tagawa. 1990. An improved $k$-$\varepsilon$ model for boundary layer flows. *J. Fluid Engng, ASME Trans.* 112:33-39.

Olson, D. A., L. R. Glicksman, and H. M. Ferm. 1990. Steady-state convection in empty and partitioned enclosures at high Rayleigh numbers. *J. Heat Transfer, ASME Trans.* 112:640-647.

Paolucci, S. 1990. Direct numerical simulation of two dimensional turbulent natural convection in an enclosed cavity. *J. Fluid Mech.* 215:229-262.

Spalding, D. B. 1994. *PHOENICS Reference Manual: TR100, TR200.* London: CHAM limited, UK.